Int. J. Solids Structures, Vol. 19, No. 2, pp. 105–119, 1983
Printed in Great Britain.

0020-7683/83/020105-15$03.00/0
Pergamon Press Ltd.

THE END PROBLEM OF A FINITE ELASTIC CYLINDER PRESSED AGAINST A ROUGH, RIGID, SLIDING SURFACE

R. J. CONANT† and R. SOLECKI
Department of Mechanical Engineering, The University of Connecticut, Storrs, CT 06268, U.S.A.

(*Received* 5 *October* 1981; *in revised form* 27 *May* 1982)

Abstract—The non-axisymmetric problem of a finite, circular, elastic cylinder, one end of which contacts a moving, rigid surface in the presence of Coulomb friction while the opposite end is constrained against in-plane displacements but subjected to a uniform normal displacement, is considered. The governing differential equations are converted to an infinite system of singular integral equations with the aid of the Papkovich-Neuber potentials and the subsequent application of multiple Fourier transformations. These are solved numerically and the components of stress and displacement at the ends of the cylinder are determined.

For the frictionless case, the solution is shown to agree closely with known results.

For the frictional case, stresses at the ends of the cylinder are given for two aspect ratios and several friction coefficients.

1. INTRODUCTION

Recent work in the field of wear testing of materials by Rice and R. Solecki[1] has led the authors to consider the problem discussed in this paper. Wear testing is accomplished by sliding a specimen of one material along a counterface, possibly of a different material. For small specimen sizes, difficulties arise in determining the interface pressure distribution experimentally, so that the analytical determination of the distribution is of practical interest.

The purpose of this paper is to determine the pressure distribution between a rough, rigid, sliding surface and one end of a finite-length right, circular cylinder, whose opposite end is constrained against in-plane displacements and given a uniform normal displacement, as shown in Fig. 1.

An interesting historical account of the cylinder problem up to 1968 can be found in de La Penha[2] and will not be repeated here. More recently, Benthem and Minderhoud[3] applied the radial eigenfunction technique to the problem of a cylinder compressed between rough rigid stamps (Filon's problem), and obtained accurate results near the circumference of the ends of the cylinder, where the stress distribution is known to be singular. Their method requires prior knowledge of the nature of the stress singularity, obtained through the solution of an auxiliary

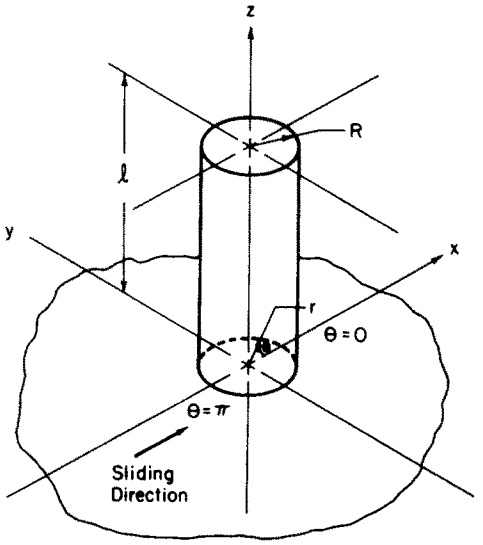

Fig. 1. Cylinder geometry.

†Present address: Department of Mechanical Engineering, Montana State University, Bozeman, MT 59715, U.S.A.

problem applicable to the local region containing the singularity. Zak[4] also determined the singular behavior of the stresses through the solution of an auxiliary problem. This solution was then matched with a finite element solution at a finite distance from the singularity. Gupta[5] used an integral transform technique to reduce the problem of a semi-infinite cylinder with one end fixed to the solution of a singular integral equation, which was solved numerically. By isolating the singular part of the kernel, the nature of the stress singularity was found directly from the integral equation.

The most recent work is that of J.S. Solecki and Swedlow[6], who developed a special 5-node finite element to model the corner. An array of these elements was then coupled to a region of "regular" finite elements to complete the modelling of the cylinder.

Very few solutions exist for the non-axisymmetric cylinder problem. Yao[7] and Steven[8] obtained solutions for infinite cylinders loaded on the lateral surface, but to the authors' knowledge no solutions exist for cylinders of finite length.

Here, a non-axisymmetric problem for a finite cylinder with loaded ends and stress-free lateral surface is converted to the solution of an infinite system of singular integral equations. This is achieved by first uncoupling the governing differential equations through use of the Papkovich–Neuber potentials and then applying finite Fourier transformations to the resulting equations. The integral equations are subsequently reduced, by the collocation method, to an infinite system of algebraic equations, which are solved by the method of reduction.

While the approach taken by Gupta can be applied to systems of integral equations[9], the complexity and number of kernels involved in the present problem make it unattractive. Instead, the approach of Benthem and Minderhoud is followed here by representing those unknown quantities that are singular as the sum of a singular part of known strength and unknown intensity and a regular part, in the form of a series.

For the frictionless case, the stresses compare very well with those of Benthem and Minderhoud. Stresses for the frictional case are given graphically for two values of aspect ratio (length/diameter) and for several friction coefficients. Stress intensities for both the radial and tangential shear stresses are given as functions of circumferential location.

2. FORMULATION†

Figure 1 shows an isotropic, homogeneous, elastic cylinder of radius R and length l. The end of the cylinder at $z = l$ is subjected to a uniform longitudinal displacement while the in-plane displacements are zero. The end of the cylinder at $z = 0$ contacts a rough, rigid surface that is moving in the x direction. The lateral surface is stress-free.

In cylindrical coordinates, the displacement components u, v, w in the r, θ, and z directions, respectively, must satisfy, in the absence of body forces, the following equations:

$$\nabla^2 u - \frac{u}{r^2} - \frac{2}{r^2}\frac{\partial v}{\partial \theta} + \frac{\lambda+\mu}{\mu}\frac{\partial \Delta}{\partial r} = 0,$$

$$\nabla^2 v - \frac{v}{r^2} + \frac{2}{r^2}\frac{\partial u}{\partial \theta} + \frac{\lambda+\mu}{\mu}\frac{1}{r}\frac{\partial \Delta}{\partial \theta} = 0,$$

$$\nabla^2 w + \frac{\lambda+\mu}{\mu}\frac{\partial \Delta}{\partial z} = 0, \tag{1a–c}$$

where the Laplacian and dilatation are, respectively:

$$\nabla^2 \equiv \frac{\partial^2}{\partial r^2} + \frac{1}{r}\frac{\partial}{\partial r} + \frac{1}{r^2}\frac{\partial^2}{\partial \theta^2} + \frac{\partial^2}{\partial z^2},$$

$$\nabla \equiv \frac{\partial u}{\partial r} + \frac{1}{r}\left(\frac{\partial v}{\partial \theta} + u\right) + \frac{\partial w}{\partial z}. \tag{2a, b}$$

†Due to space limitations, many lengthy expressions that arose during the course of the analysis are not presented here. The interested reader should consult Ref.[11].

The boundary conditions appropriate to the problem are

$$\sigma_{rr}(R, \theta, z) = \sigma_{r\theta}(R, \theta, z) = \sigma_{rz}(R, \theta, z) = 0, \tag{3a–c}$$

$$u(r, \theta, l) = v(r, \theta, l) = 0,$$
$$w(r, \theta, l) = -\hat{W}, \tag{4a–c}$$

$$\sigma_{xz}(x, y, 0) = \sigma_{rz}(r, \theta, 0)\cos\theta - \sigma_{\theta z}(r, \theta, 0)\sin\theta = k\sigma_{zz}(r, \theta, 0),$$
$$\sigma_{yz}(x, y, 0) = \sigma_{rz}(r, \theta, 0)\sin\theta + \sigma_{\theta z}(r, \theta, 0)\cos\theta = 0,$$
$$w(r, \theta, 0) = 0, \tag{5a–c}$$

where k is the coefficient of sliding friction, and $\hat{W}$ is a constant. Coulomb friction is assumed.

The x-z plane of the cylinder is a plane of symmetry on which the following conditions apply:

$$\sigma_{r\theta}(r, {}^{0}_{\pi}, z) = \sigma_{z\theta}(r, {}^{0}_{\pi}, z) = 0,$$
$$v(r, {}^{0}_{\pi}, z) = 0. \tag{6a–c}$$

In addition, it is required that the displacements remain bounded at the origin.

The Papkovich–Neuber potential functions are used to partially uncouple eqns (1). In cylindrical coordinates, these are defined by:†

$$u = \frac{\partial}{\partial r}(\phi + r\psi_r) - 4(1-\nu)\psi_r,$$
$$v = \frac{1}{r}\frac{\partial}{\partial\theta}(\phi + r\psi_r) - 4(1-\nu)\psi_\theta,$$
$$w = \frac{\partial}{\partial z}(\phi + r\psi_r), \tag{7a–c}$$

where ν is Poisson's ratio.

When these are substituted into (1), the following equations defining the potential functions result:

$$\nabla^2\phi = 0,$$
$$\nabla^2\psi_r - \frac{1}{r^2}\psi_r - \frac{2}{r^2}\frac{\partial\psi_\theta}{\partial\theta} = 0,$$
$$\nabla^2\psi_\theta - \frac{1}{r^2}\psi_\theta + \frac{2}{r^2}\frac{\partial\psi_r}{\partial\theta} = 0. \tag{8a–c}$$

The stress components are given in terms of the potential functions in Ref. [11].

While the introduction of potential functions leads to a set of equations that is at least partially uncoupled, the resulting boundary conditions are more complicated. The substitution of (7) into (3)–(6) results in the following conditions:

$$\left.\begin{aligned}
&\frac{\partial^2\phi}{\partial r^2} + r\frac{\partial^2\psi_r}{\partial r^2} - 2(1-\nu)\frac{\partial\psi_r}{\partial r} - 2\nu\frac{1}{r}\left(\psi_r + \frac{\partial\psi_\theta}{\partial\theta}\right) = 0, && r = R\\
&-\frac{1}{r^2}\frac{\partial\phi}{\partial\theta} + \frac{1}{r}\frac{\partial^2\phi}{\partial r\partial\theta} + \frac{\partial^2\psi_r}{\partial r\partial\theta} - 2(1-\nu)\left(\frac{\partial\psi_\theta}{\partial r} - \frac{1}{r}\psi_\theta + \frac{1}{r}\frac{\partial\psi_r}{\partial\theta}\right) = 0, && 0 \le \theta \le \pi\\
&\frac{\partial^2\phi}{\partial r\partial z} + r\frac{\partial^2\psi_r}{\partial r\partial z} + \frac{\partial\psi_r}{\partial z} - 2(1-\nu)\frac{\partial\psi_r}{\partial z} = 0, && 0 \le z \le l
\end{aligned}\right\} \tag{9a–c}$$

†Eubanks and Sternberg[10] have shown that, for convex regions, any component of the vector potential, $\underset{\sim}{\psi}$, may be chosen as zero without affecting completeness. In this problem, $\psi_z = 0$ was chosen.

$$\left.\begin{aligned}
&\frac{\partial}{\partial r}(\phi + r\psi_r) - 4(1-\nu)\psi_r = 0,\\
&\frac{1}{r}\frac{\partial}{\partial\theta}(\phi + r\psi_r) - 4(1-\nu)\psi_\theta = 0,\\
&\frac{\partial}{\partial z}(\phi + r\psi_r) = -\hat{W},
\end{aligned}\right\} \quad 0 \le r \le R;\ 0 \le \theta \le \pi;\ z = l \tag{10a-c}$$

$$\left.\begin{aligned}
&\frac{\partial}{\partial z}(\phi + r\psi_r) = 0, && 0 \le \theta \le R\\
&\frac{\partial\psi_r}{\partial z}\sin\theta + \frac{\partial\psi_\theta}{\partial z}\cos\theta = 0, && 0 \le \theta \le R\\
&4(1-\nu)\left(\frac{\partial\psi_r}{\partial z}\cos\theta - \frac{\partial\psi_\theta}{\partial z}\sin\theta\right) + 2k\left\{\frac{\partial^2}{\partial z^2}(\phi + r\psi_r)\right. && 0 \le \theta \le \pi\\
&\qquad \left. - 2\nu\frac{1}{r}\left[\frac{\partial}{\partial r}(r\psi_r) + \frac{\partial\psi_\theta}{\partial\theta}\right]\right\} = 0, && z = 0
\end{aligned}\right\} \tag{11a-c}$$

$$\frac{\partial\phi}{\partial\theta} = \frac{\partial\psi_r}{\partial\theta} = \psi_\theta = 0, \quad 0 \le r \le R;\ \theta = 0,\ \pi;\ 0 \le z \le l. \tag{12a-c}$$

In addition, the expressions for the displacements, eqns (7), must remain bounded at $r = 0$.

Equations (8)–(12) define a boundary value problem in terms of the potential functions. Once solved, the corresponding displacements and stresses can be readily determined from equations given in[11].

3. REDUCTION OF THE PROBLEM TO A SYSTEM OF INTEGRAL EQUATIONS

The problem can be solved using integral transformations by defining the following transforms:

$$\bar{\bar{\phi}}(r, n, m) \equiv \int_0^l \int_0^\pi \phi(r, \theta, z)\cos n\theta \cos\lambda_m z\, d\theta\, dz, \qquad \begin{matrix} 0 \le r \le R \\ m, n = 0, 1, 2, \ldots \end{matrix}$$

$$\bar{\bar{\psi}}_r(r, n, m) \equiv \int_0^l \int_0^\pi \psi_r(r, \theta, z)\cos n\theta \cos\lambda_m z\, d\theta\, dz, \qquad \begin{matrix} 0 \le r \le R \\ m, n = 0, 1, 2, \ldots \end{matrix}$$

$$\bar{\bar{\psi}}_\theta(r, n, m) \equiv \int_0^l \int_0^\pi \psi_\theta(r, \theta, z)\sin n\theta \cos\lambda_m z\, d\theta\, dz, \qquad \begin{matrix} 0 \le r \le R \\ n = 1, 2, \ldots \\ m = 0, 1, 2, \ldots \end{matrix} \tag{13a-c}$$

where $\lambda_m = m\pi/l$. After transformation, eqns (8) become:†

$$\frac{d^2\bar{\bar{\phi}}(r, n, m)}{dr^2} + \frac{1}{r}\frac{d\bar{\bar{\phi}}(r, n, m)}{dr} - \left(\frac{n^2}{r^2} + \lambda_m^2\right)\bar{\bar{\phi}}(r, n, m)$$
$$= -r\hat{G}_{1n}(r) + (-1)^m[\pi\hat{W}\delta_{0n} + r\hat{G}_{2n}(r)], \quad \begin{matrix} 0 \le r \le R \\ n, m = 0, 1, 2, \ldots \end{matrix}$$

$$\frac{d^2\bar{\bar{\psi}}_r(r, n, m)}{dr^2} + \frac{1}{r}\frac{d\bar{\bar{\psi}}_r(r, n, m)}{dr} - \left(\frac{n^2}{r^2} + \lambda_m^2\right)\bar{\bar{\psi}}_r(r, n, m) - \frac{1}{r^2}\bar{\bar{\psi}}_r(r, n, m)$$
$$- 2\frac{n}{r^2}\bar{\bar{\psi}}_\theta(r, n, m) = \hat{G}_{1n}(r) - (-1)^m\hat{G}_{2n}(r), \quad \begin{matrix} 0 \le r \le R \\ n, m = 0, 1, 2, \ldots \end{matrix}$$

†Equations (10c), (11a) have been used in obtaining (14a).

$$\frac{d^2\bar{\phi}_\theta(r,n,m)}{dr^2}+\frac{1}{r}\frac{d\bar{\psi}_\theta(r,n,m)}{dr}-\left(\frac{n^2}{r^2}+\lambda_m^2\right)\bar{\psi}_\theta(r,n,m)-\frac{1}{r^2}\bar{\psi}_\theta(r,n,m)$$

$$-2\frac{n}{r^2}\bar{\psi}_r(r,n,m)=\hat{G}_{3n}(r)-(-1)^m\hat{G}_{4n}(r),\quad 0\le r\le R$$

$$n=1,2,\ldots$$

$$m=0,1,2,\ldots \qquad (14a\text{–}c)$$

where δ_{mn} is the Kronecker delta.

The auxiliary functions $\hat{G}_{in}(r)$, etc. are as yet undetermined. However, they are related to the shear stress components at the ends of the cylinder as follows:

$$\eta\bar{\sigma}_{rz}(r,n,0)=-2(1-\nu)\hat{G}_{1n}(r),\quad n=0,1,2,\ldots$$

$$\eta\bar{\sigma}_{rz}(r,n,l)=-2(1-\nu)\hat{G}_{2n}(r),\quad n=0,1,2,\ldots$$

$$\eta\bar{\sigma}_{\theta z}(r,n,0)=-2(1-\nu)\hat{G}_{3n}(r),\quad n=1,2,\ldots$$

$$\eta\bar{\sigma}_{\theta z}(r,n,l)=-2(1-\nu)\hat{G}_{4n}(r),\quad n=1,2,\ldots \qquad (15a\text{–}d)$$

where

$$\bar{\sigma}_{rz}(r,n,a)\equiv\int_0^\pi \sigma_{rz}(r,\theta,a)\cos n\theta\,d\theta,\quad n=0,1,2,\ldots$$

$$\bar{\sigma}_{\theta z}(r,n,a)\equiv\int_0^\pi \sigma_{\theta z}(r,\theta,a)\sin n\theta\,d\theta,\quad n=1,2,\ldots \qquad (16a,b)$$

$$\eta\equiv\frac{1+\nu}{E}, \qquad (17)$$

and E is Young's modulus.

Equations (14b, c) can be uncoupled, for $n>0$, by first adding and then subtracting to give equations for $\bar{\psi}_r+\bar{\psi}_\theta$ and $\bar{\psi}_r-\bar{\psi}_\theta$.† These and eqn (14a) are Euler's equations for $m=0$ and modified Bessel's equations for $m>0$. Five separate combinations of m and n have to be considered, and the solutions yielding bounded displacements at the origin are given as:‡

n = m = 0:

$$\bar{\phi}(r,0,0)=\bar{\phi}_p(r,0,0),$$

$$\bar{\psi}_r(r,0,0)=B_0r+\bar{\psi}_{rp}(r,0,0), \qquad (18a,b)$$

n = 1; m = 0:

$$\bar{\phi}(r,1,0)=A_3r+\bar{\phi}_p(r,1,0),$$

$$\bar{\psi}_r(r,1,0)=C_1r^2+D_2+\bar{\psi}_{rp}(r,1,0),$$

$$\bar{\psi}_\theta(r,1,0)=C_1r^2-D_2+\bar{\psi}_{\theta p}(r,1,0), \qquad (19a\text{–}c)$$

n = 2, 3, . . . ; m = 0

$$\bar{\phi}(r,n,0)=A_{3n}r^n+\bar{\phi}_p(r,n,0),$$

$$\bar{\psi}_r(r,n,0)=A_{1n}r^{n+1}+B_{1n}r^{n-1}+\bar{\psi}_{rp}(r,n,0),$$

$$\bar{\psi}_\theta(r,n,0)=A_{1n}r^{n+1}-B_{1n}r^{n-1}+\bar{\psi}_{\theta p}(r,n,0), \qquad (20a\text{–}c)$$

n = 0; m = 1, 2, . . .

$$\bar{\phi}(r,0,m)=D_mI_0(\lambda_mr)+\bar{\phi}_p(r,0,m),$$

$$\bar{\psi}_r(r,0,m)=B_mI_1(\lambda_mr)+\bar{\psi}_{rp}(r,0,m), \qquad (21a,b)$$

n, m = 1, 2, . . .

$$\bar{\phi}(r,n,m)=C_{3nm}I_n(\lambda_mr)+\bar{\phi}_p(r,n,m),$$

$$\bar{\psi}_r(r,n,m)=C_{1nm}I_{n-1}(\lambda_mr)+C_{2nm}I_{n+1}(\lambda_mr)+\bar{\psi}_{rp}(r,n,m),$$

$$\bar{\psi}_\theta(r,n,m)=-C_{1nm}I_{n-1}(\lambda_mr)+C_{2nm}I_{n+1}(\lambda_mr)+\bar{\psi}_{\theta p}(r,n,m). \qquad (22a\text{–}c)$$

The subscript p appearing in certain terms indicates particular solutions, given in[11].

†See Ref. ([12], p. 239).

‡Certain constants appearing in these solutions have been chosen as zero because only their derivatives appear in the transformed displacement expressions.

The constants contained in (18)–(22) are found by first transforming the boundary conditions on the lateral surface, eqns (9), and then substituting the above expressions into the resulting equations. This leads, in general, to a system of 3 algebraic equations and 3 unknowns for each value of n, m, from which the constants can be determined. After lengthy algebraic manipulations, the constants are found to be:

$$B_0 = \frac{1}{4}\pi\hat{W} - U_1(R,0,0) + (1-2\nu)\frac{1}{R^2}U_2(R,0,0) \tag{23}$$

$$C_1 = -\frac{1}{2}U_1(R,1,0) + \frac{1}{2}(5-4\nu)R^{-4}U_2(R,1,0) + \frac{1}{4}(1-2\nu)R^{-2}U_3(R,1,0) + R^{-4}U_6(R,1,0) \tag{24}$$

$$A_{1n} = -\frac{1}{2}U_1(R,n,0) + \frac{1}{2}[n+4(1-\nu)]R^{-2(n+1)}U_2(R,n,0)$$
$$+\frac{1}{2}(n-1)R^{-2n}U_4(R,n,0) + nR^{-2(n+1)}U_6(R,n,0), \quad n = 2,3,\ldots$$

$$C_{1n} = -\frac{1}{2}(n+1)[n+4(1-\nu)]R^{-2n}U_2(R,n,0) - \frac{1}{2}[n-4(1-\nu)]U_3(R,n,0)$$
$$-\frac{1}{2}n^2R^{-2(n-1)}U_4(R,n,0) - nU_5(R,n,0)$$
$$-n(n+1)R^{-2n}U_6(R,n,0), \quad n = 2,3,\ldots \tag{25a, b}$$

where $C_{1n} \equiv nA_{3n} + [n-4(1-\nu)]B_{1n}$ and $U_1(R,0,0)$, etc. are the particular integrals given in[11]. Also, for $m > 0$:

$$B_m = -U_1(R,0,m) + \frac{1}{C_m}\left\{[2(1-\nu)+\gamma_m^2]\frac{\gamma_m}{R^2}I_1K_1 + \frac{\gamma_m^3}{R^2}I_0K_0\right.$$
$$\left.+2(1-\nu)\frac{\gamma_m}{R^2}\right\}U_2(R,0,m) + \frac{1}{C_m}\frac{\gamma_m^2}{R^3}U_4(R,0,m), \quad m = 1,2,\ldots$$

$$D_m = \frac{1}{C_m}[2(1-\nu)(1-2\nu)-\gamma_m^2]\frac{1}{R}U_2(R,0,m) - U_3(R,0,m)$$
$$+\frac{1}{C_m}\left\{-[2(1-\nu)+\gamma_m^2]\frac{\gamma_m}{R^2}I_1K_1 - \frac{\gamma_m^3}{R^2}I_0K_0 + 2(1-\nu)\frac{\gamma_m}{R^2}\right\}$$
$$\times U_4(R,0,m) - \frac{R^2}{\gamma_m^2}(-1)^m\pi\hat{W}, \quad m = 1,2,\ldots, \tag{26a, b}$$

where

$$C_m \equiv \frac{\gamma_m}{R^2}\{[2(1-\nu)+\gamma_m^2]I_1^2 - \gamma_m^2I_0^2\}, \quad m = 1,2,\ldots \tag{27}$$

$$\gamma_m \equiv \lambda_m R. \tag{28}$$

It is understood that the argument of I_n, K_n is γ_m, unless stated otherwise. For m, n both greater than zero, the constants can be expressed as:

$$C_{inm} = \Sigma_{j=1}^{6}Z_{ij}(n,m)U_j(R,n,m), \quad n,m = 1,2,\ldots \quad i = 1,2,3. \tag{29}$$

The quantities $Z_{ij}(n,m)$ are given in[11]. In addition to eqn (24), the transformed boundary conditions on the lateral surface for $n = 1$, $m = 0$ yield the following condition:

$$\int_0^R [\hat{G}_{11}(s) - \hat{G}_{21}(s) - \hat{G}_{31}(s) + \hat{G}_{41}(s)]s\,ds = 0. \tag{30}$$

This equation simply states that, since the lateral surface is stress free and no shear stresses act on the plane of symmetry, the shear stresses acting on the ends of the cylinder must maintain its static equilibrium in the x-direction.

The following equations result upon elimination of θ from the remaining boundary conditions at the ends of the cylinder, eqns (10a, b) and (11b, c):

n = 0:

$$\frac{\partial}{\partial r}[\bar{\phi}(r,0,l)+r\bar{\psi}_r(r,0,l)]-4(1-\nu)\bar{\psi}_r(r,0,l)=0,$$

$$2(1-\nu)[\hat{G}_{11}(r)-\hat{G}_{31}(r)]+k\left\{\frac{\partial^2}{\partial z^2}[\bar{\phi}(r,0,0)+r\bar{\psi}_r(r,0,0)]\right.$$

$$\left.-2\nu\frac{1}{r}\frac{\partial}{\partial r}[r\bar{\psi}_r(r,0,0)]\right\}=0, \tag{31a, b}$$

n = 1, 2, ...

$$\frac{\partial}{\partial r}[\bar{\phi}(r,n,l)+r\bar{\psi}_r(r,n,l)]-4(1-\nu)\bar{\psi}_r(r,n,l)=0,$$

$$\frac{n}{r}[\bar{\phi}(r,n,l)+r\bar{\psi}_r(r,n,l)]+4(1-\nu)\bar{\psi}_\theta(r,n,l)=0,$$

$$\hat{G}_{1,n-1}(r)-\hat{G}_{1,n+1}(r)+(1-\delta_{1n})\hat{G}_{3,n-1}(r)+\hat{G}_{3,n+1}(r)=0,$$

$$(1-\nu)[\hat{G}_{1,n-1}(r)+\hat{G}_{1,n+1}(r)+(1-\delta_{1n})\hat{G}_{3,n-1}(r)-\hat{G}_{3,n+1}(r)]$$

$$+k\left\{\frac{\partial^2}{\partial z^2}[\bar{\phi}(r,n,0)+r\bar{\psi}_r(r,n,0)-2\nu\frac{1}{r}\left\{\frac{\partial}{\partial r}[r\bar{\psi}_r(r,n,0)\right.\right.$$

$$\left.\left.+n\bar{\psi}_\theta(r,n,0)\right\}\right\}=0. \tag{32a–d}$$

The double-barred quantities can be introduced in (31), (32) via the inversion formula for the finite Fourier cosine transform.† Expressions (18)–(22) and (23)–(29) are then substituted in the resulting equations, and the order of summation and integration interchanged. These equations contain integrals from 0 to r and 0 to R which can be combined so that only the latter remain. This leads to the following coupled, infinite system of Fredholm integral equations:

$$\left.\begin{aligned}
&\int_0^\tau G_{10}(\xi)\kappa_1(\rho,\xi)\,d\xi+\int_0^\tau G_{20}(\xi)\kappa_2(\rho,\xi)\,d\xi=-\nu\rho,\\
&2(1-\nu)[G_{11}(\rho)-G_{31}(\rho)]+k\int_0^\tau G_{10}(\xi)\kappa_3(\rho,\xi)\,d\xi+k\int_0^\tau G_{20}(\xi)\kappa_4(\rho,\xi)\,d\xi=k(1+\nu),\\
&G_{1,n-1}(\rho)-G_{1,n+1}(\rho)+(1-\delta_{1n})G_{3,n-1}(\rho)+G_{3,n+1}(\rho)=0,\quad n=1,2,\ldots\\
&\Sigma_{j=1}^4\left[\int_0^\tau G_{jn}(\xi)\kappa_{j,n}^i(\rho,\xi)\,d\xi\right]+\delta_{1n}A_0=0,\quad n=1,2,\ldots\\
&\qquad\qquad\qquad\qquad\qquad\qquad\qquad\qquad\qquad\qquad i=1,2\\
&2(1-\nu)[G_{1,n+1}(\rho)-G_{3,n+1}(\rho)]+k\Sigma_{j=1}^4\left[\int_0^\tau G_{jn}(\xi)\kappa_{j,n}^3(\rho,\xi)\,d\xi\right]=0,\quad n=1,2,\ldots
\end{aligned}\right\}\ (0\le\rho<\tau) \tag{33a–e}$$

where

$$A_0\equiv\frac{1}{l^2}[A_3-(3-4\nu)D_2],\quad \rho\equiv\frac{r}{l},\quad \xi\equiv\frac{s}{l},\quad \tau\equiv\frac{R}{l},\quad G_{in}(\rho)\equiv\frac{l\hat{G}_{in}(\rho)}{\pi\hat{W}}. \tag{34}$$

†Because of the second derivative with respect to z, this involves differentiation of the Fourier sine series which, in general, is not differentiable term-by-term. See ([13], pp. 137–143).

The kernels of the integral equations (33) are given by:

$$\left.\begin{aligned}
\kappa_1(\rho,\xi) &\equiv \xi[A_1(\rho,\xi)+2\Sigma_{m=1}^{\infty}(-1)^m B_{1,m}(\rho,\xi)],\\
\kappa_2(\rho,\xi) &\equiv -\xi[A_1(\rho,\xi)+2\Sigma_{m=1}^{\infty}B_{1,m}(\rho,\xi)],\\
\kappa_3(\rho,\xi) &\equiv -[A_2(\rho,\xi)+2\Sigma_{m=1}^{\infty}\xi B_{2,m}(\rho,\xi)],\\
\kappa_4(\rho,\xi) &\equiv [A_2(\rho,\xi)+2\Sigma_{m=1}^{\infty}(-1)^m\xi B_{2,m}(\rho,\xi)],
\end{aligned}\right\} \quad 0\le(\xi,\rho)\le\tau \tag{35a-d}$$

$$\left.\begin{aligned}
\kappa^i_{j,n}(\rho,\xi) &\equiv \xi[A^i_{1/2(j+1),n}(\rho,\xi)+2\Sigma_{m=1}^{\infty}(-1)^m B^i_{1/2(j+1),mn}(\rho,\xi), \quad i=1,2\\
\kappa^i_{j+1,n}(\rho,\xi) &\equiv -\xi[A^i_{1/2(j+1),n}(\rho,\xi)+2\Sigma_{m=1}^{\infty}B^i_{1/2(j+1),mn}(\rho,\xi)], \quad i=1,2\\
\kappa^3_{j,n}(\rho,\xi) &\equiv -[A^3_{1/2(j+1),n}(\rho,\xi)+2\Sigma_{m=1}^{\infty}\xi B^3_{1/2(j+1),mn}(\rho,\xi)],\\
\kappa^3_{j+1,n}(\rho,\xi) &\equiv [A^3_{1/2(j+1),n}(\rho,\xi)+2\Sigma_{m=1}^{\infty}(-1)^m\xi B^3_{1/2(j+1),mn}(\rho,\xi)],
\end{aligned}\right\} \quad \begin{aligned}&0\le(\xi,\rho)\le\tau\\&j=1,3\\&n=1,2,\ldots\end{aligned} \tag{36a-d}$$

The quantities appearing in (35), (36) are defined in[11].

The $4n+2$ equations (33) contain $4n+3$ unknowns (A_0, G_{10}, G_{20}, G_{jn}, $j=1-4$, $n=1,2,\ldots$). The additional equation needed to solve the system is provided by (30) which, on introducing the dimensionless quantities (34), becomes:

$$\int_0^{\tau}[G_{11}(\xi)-G_{21}(\xi)-G_{31}(\xi)+G_{41}(\xi)]\xi\,d\xi=0. \tag{37}$$

For the frictionless case ($k=0$) eqns (33) reduce to the single integral equation:

$$\int_0^{\tau}G_{20}(\xi)\kappa_2(\rho,\xi)\,d\xi=-\nu\rho, \quad 0\le\rho<\tau. \tag{38}$$

For large values of the summation index, the modified Bessel functions appearing in the infinite series of eqns (35), (36) can be replaced by their asymptotic formulae. From the resulting asymptotic expressions it can be seen that certain of the positive series (including the one in κ_2) diverge when $(2\tau-\rho-\xi)=0$ and $|\rho-\xi|=0$. Thus, certain kernels and, hence, the system of integral equations (33) are singular.

Once the integral equations are solved, stresses and displacements at any point in the cylinder can be found. However, because of the length of these expressions, the stresses and displacements at the ends of the cylinder are given in[11]. Also, the complete expressions for stresses and displacements in terms of the auxiliary functions can be found in[11].

4. SOLUTION OF THE INTEGRAL EQUATION—FRICTIONLESS CASE

It is well known that, at the end of the cylinder constrained against in-plane displacements, both the normal and shear stress components become infinite as the circumference is approached. This singular behavior is characterized by

$$\lim_{\rho\to\tau}\sigma=\frac{c}{(1-\rho/\tau)^{\lambda}}, \tag{39}$$

where the strength of the singularity, λ, satisfies the characteristic equation[3]:

$$\cos^2\left(\lambda\frac{\pi}{2}\right)=\frac{4(1-\nu)^2}{3-4\nu}-\frac{(1-\lambda)^2}{3-4\nu} \tag{40}$$

and c is the stress intensity coefficient.†

†This terminology has been chosen to avoid possible confusion with the well-established meaning of "stress intensity factor" in linear fracture mechanics.

For $\nu = 0.25$, λ is given as [3]:

$$\lambda = 0.25525. \tag{41}$$

The integral equation (38) can be solved by the collocation method. Following Benthem and Minderhoud [3], the singularity contained in $G_{20}(\rho)$ is accounted for explicitly. The numerical integration is carried out using Simpson's rule. Because the kernel is singular, the length of the subinterval in the region near the point $\xi = \rho$ is chosen much smaller than for other regions, and the integration is performed over the range $0 \le \xi \le (\rho - \epsilon)$ and $(\rho + \epsilon) \le \xi \le \tau$. The integral between $(\rho - \epsilon)$ and $(\rho + \epsilon)$ is evaluated as the sum of two rectangular areas, using the values of the integrand at $(\rho - \epsilon)$ and $(\rho + \epsilon)$. Tests have been run for several values of ϵ and it has been found that the solution is stable for $\epsilon \lesssim 0.0005\rho$.

Three different forms have been used for $G_{20}(\rho)$:

$$G_{20}(\rho) \approx b_1 f_\infty(\rho) + \Sigma_{i=2}^{N} b_i J_1\left(\beta_{i-1}\frac{\rho}{\tau}\right) \tag{42}$$

$$G_{20}(\rho) \approx b_1 f_\infty(\rho) + \Sigma_{i=2}^{N} b_i \cos(i-2)\pi\frac{\rho}{\tau} \tag{43}$$

$$G_{20}(\rho) \approx \frac{\Sigma_{i=1}^{N} b_i \cos(i-1)\pi\dfrac{\rho}{\tau}}{(\tau-\rho)^{\lambda}} \tag{44}$$

where $J_1(\beta_i) = 0$, $i = 1, 2, \ldots$

$$f_\infty(\rho) \equiv \left(1-\frac{\rho}{\tau}\right)^{-\lambda} - \left(1-\frac{\rho}{\tau}\right) - \frac{1}{2}\lambda(\lambda+1)\rho\tau^{-\lambda}(\rho-\tau). \tag{46}$$

Equation (42) is that used in [3].

For eqns (42), (43) the radial stress intensity coefficient is:

$$K_r \equiv -2(1-\nu)b_1 \tag{47}$$

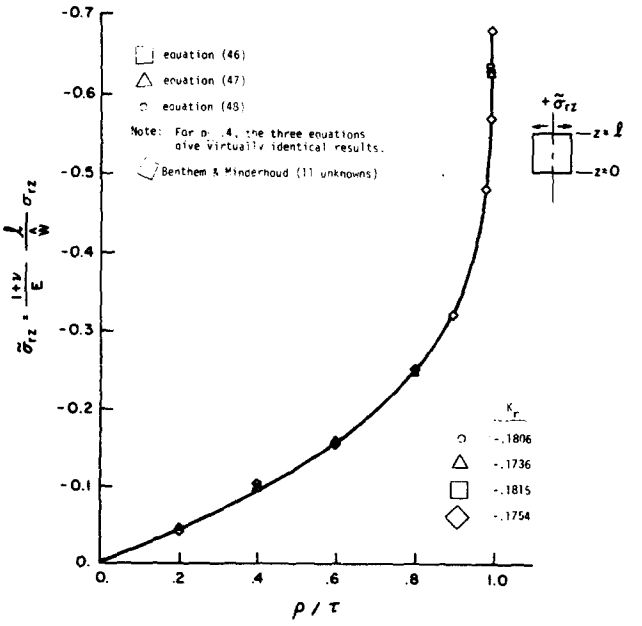

Fig. 2. Shear stress distribution at $z = l$ for various basis functions. Frictionless case. $l/D = 1$, $\nu = 0.25$.

and for eqn (44),

$$K_r \equiv -2(1-\nu)\Sigma_{i=1}^{N}(-1)^{i-1}b_i. \tag{48}$$

The resulting radial shear stress distribution at $z = l$, using 5 collocation points, is given in Fig. 2 for $l/D = 1$, $\nu = 0.25$. The stress distribution obtained by Benthem and Minderhoud[3] results from a unit normal pressure while that obtained here is for a unit displacement. Therefore the results obtained in[3] have been multiplied by

$$\sigma_w = \frac{1}{\frac{1}{2}\tau^2}\int_0^{\tau} \tilde{\sigma}_{zz}(\rho, 0)\rho \, d\rho, \tag{49}$$

the average pressure required to produce a unit displacement in the half-cylinder.

Because the stress intensity coefficient obtained from eqn (43) gives the best correlation with that of[3], subsequent results are based on (43).

5. SOLUTION OF THE INTEGRAL EQUATIONS—FRICTIONAL CASE

Due to the frictional boundary condition, as was shown in[14], the stresses are singular also at the leading edge of the cylinder at $z = 0$. The strength of the singularity is a function of θ.

Recalling that $G_{1n}(\rho)$, $G_{3n}(\rho)$, $G_{2n}(\rho)$ and $G_{4n}(\rho)$ are related to the radial and tangential components of shear stress at $z = 0$ and $z = l$ respectively, the following forms of the auxiliary functions are used for the frictional case:

$$G_{1n}(\rho) \approx -\frac{\eta}{2(1-\nu)}\int_0^{\pi} \frac{A(\theta)}{(1-\rho/\tau)^{\lambda_1(\theta)}} \cos n\theta \, d\theta + \Sigma_{i=2}^{N} a_{in} \cos[(i-1)\pi\rho/\tau], \quad n = 0, 1, 2, \ldots$$

$$G_{2n}(\rho) \approx b_{1n} f_{\infty}(\rho) + \Sigma_{i=2}^{N} b_{in} \cos[(i-1)\pi\rho/\tau], \quad n = 0, 1, 2, \ldots$$

$$G_{3n}(\rho) \approx -\frac{\eta}{2(1-\nu)}\int_0^{\pi} \frac{B(\theta)}{(1-\rho/\tau)^{\lambda_1(\theta)}} \sin n\theta \, d\theta + \Sigma_{i=2}^{N} c_{in} \cos[(i-1)\pi\rho/\tau], \quad n = 1, 2, \ldots$$

$$G_{4n}(\rho) \approx d_{1n} f_{\infty}(\rho) + \Sigma_{i=2}^{N} d_{in} \cos[(i-1)\pi\rho/\tau], \quad n = 1, 2, \ldots \tag{50a–d}$$

The stress intensity coefficients for shear stresses at $z = l$ are:

$$K_r(\theta) = -2(1-\nu)[b_{11} + 2\Sigma_{n=1}^{\infty} b_{1n} \cos n\theta]$$

$$K_\theta(\theta) = -4(1-\nu)\Sigma_{n=1}^{\infty} d_{1n} \sin n\theta \tag{51a, b}$$

The strength of the singularity at $z = 0$, $\lambda_1(\theta)$, is found as the solution of the following transcendental equation[14]:

$$2(1-\nu)\lambda_1\pi - k(1-2\nu)\cos\theta\cos\lambda_1\pi - k\cos\theta[2\lambda_1^2 + 4(2-\nu)\lambda_1 + 7 - 6\nu] = 0. \tag{52}$$

The stress intensity coefficients for shear stresses at $z = 0$ are also expanded into Fourier series

$$A(\theta) = A_0 + 2\Sigma_{m=1}^{\infty} A_m \cos m\theta, \quad B(\theta) = \Sigma_{m=1}^{\infty} B_m \sin m\theta. \tag{53}$$

In the present calculations only the first term in each of the series (53) was retained.

The asymptotic behavior of shear stresses is represented by:

$$\lim_{\rho\to\tau} \tilde{\sigma}_{rz}(\rho, \theta, l) = \frac{K_r(\theta)}{(1-\rho/\tau)^{\lambda}}, \quad \lim_{\rho\to\tau} \tilde{\sigma}_{\theta z}(\rho, \theta, l) = \frac{K_\theta(\theta)}{(1-\rho/\tau)^{\lambda}}$$

$$\lim_{\rho\to\tau} \tilde{\sigma}(\rho, \theta, 0) = \frac{A(\theta)}{(1-\rho/\tau)^{\lambda_1(\theta)}}, \quad \lim_{\rho\to\tau} \tilde{\sigma}_{\theta z}(\rho, \theta, 0) = \frac{B(\theta)}{(1-\rho/\tau)^{\lambda_1(\theta)}}. \tag{54a, b}$$

On substituting eqns (50), the system of eqns (33), (37), is reduced to an infinite system of algebraic equations, which is then solved by the reduction method.

In applying the reduction method to this problem, it has been found that if the system of equations is truncated when $n = P$, then accurate values are obtained for the first $P - 1$ auxiliary functions.

The value of P required to give accurate results for the non-axisymmetric behavior depends on l/D. For l/D of 0.1 and 1.0, $P = 4$ is sufficient, while for $l/D = 5$, P must be increased to 8.

Figures 3–8 show the normal and shear stresses at the ends of the cylinder, at $\theta = 0$ and π, for two aspect ratios and several friction coefficients. The shear stresses shown are σ_{xz} rather than σ_{rz}, in order to maintain a continuous slope at the origin. The calculated shear stresses at $z = 0$ agree, for the first four significant figures, with those obtained from multiplying the normal stress by the friction coefficient and therefore are not shown in the figures.

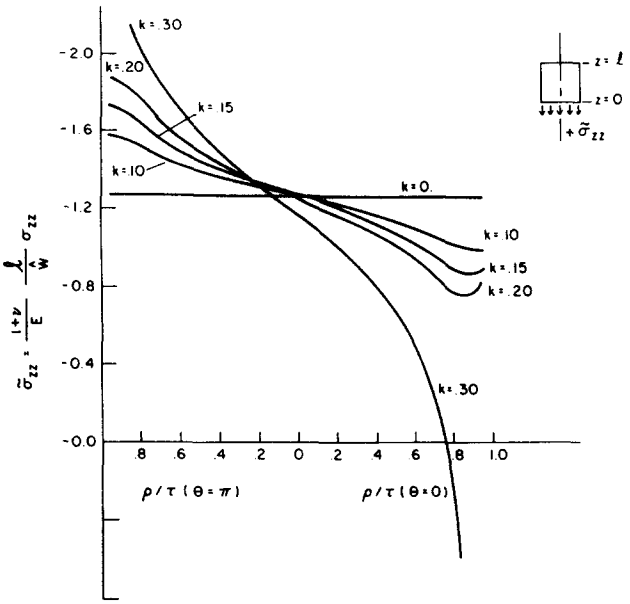

Fig. 3. Normal stress distribution at $z = 0$ for various friction coefficients. $l/D = 1$, $\nu = 0.25$.

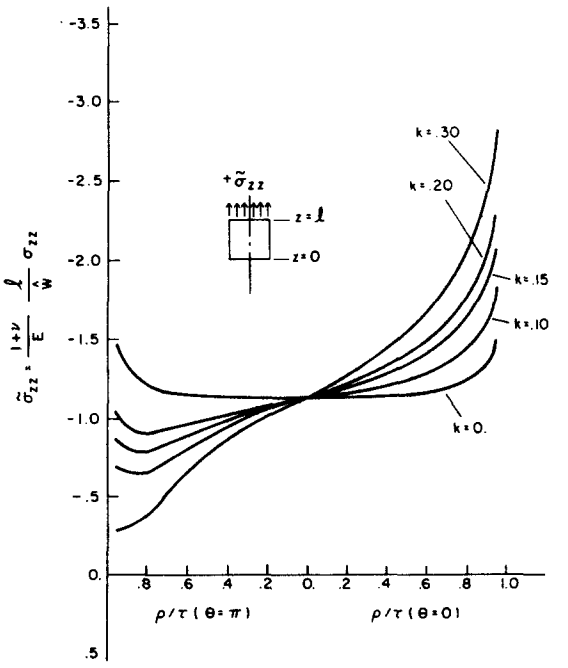

Fig. 4. Normal stress distribution at $z = l$ for various friction coefficients. $l/D = 1$, $\nu = 0.25$.

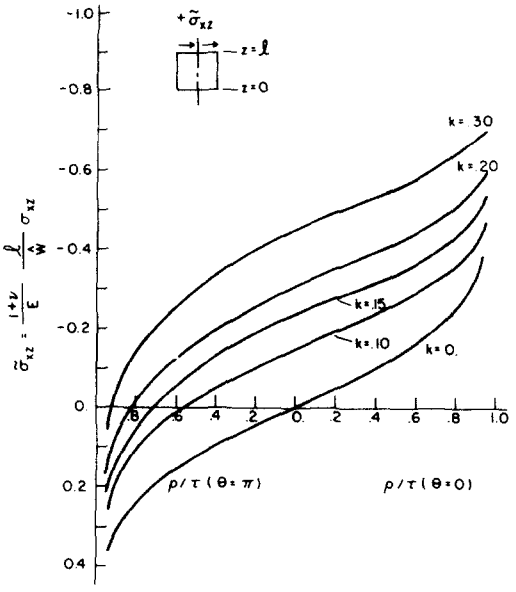

Fig. 5. Shear stress distribution at $z = l$ for various friction coefficients. $l/D = 1$, $\nu = 0.25$.

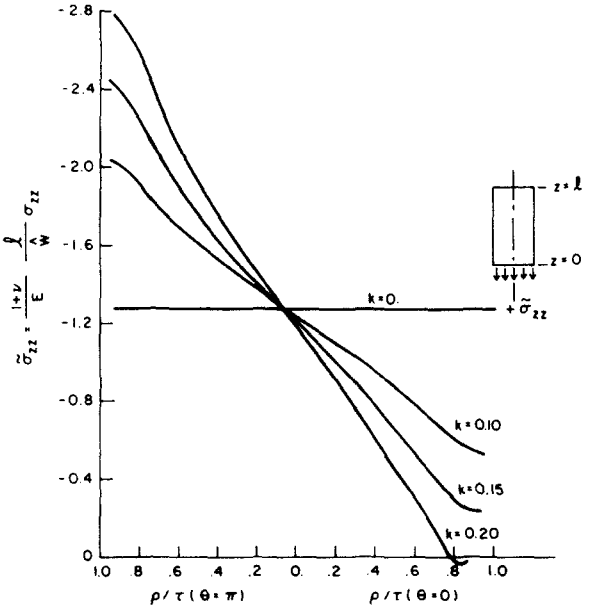

Fig. 6. Normal stress distribution at $z = 0$ for various friction coefficients. $l/D = 2$, $\nu = 0.25$.

In Fig. 5, note that at $\theta = 0$, as the friction coefficient increases, resulting in increased bending of the cylinder, the slope of the curves decreases near $\rho = \tau$ and, for large friction coefficients, the shear stress curve extends to positive infinity. At $\theta = \pi$, the slope of the curves increases near the outer radius as the friction coefficient increases. This behavior is also seen in the stress intensity coefficients for σ_{rz} at $z = l$, shown in Table 1, indicating that near the circumference, at $\theta = 0$, the shear stress is directed toward the center of the cylinder but its magnitude decreases as the overall bending increases. As the bending increases further, the shear stress is directed away from the center, and its magnitude increases. At $\theta = \pi$, the shear stress is directed toward the center and as the overall bending in the cylinder decreases, the magnitude of σ_{xz} increases.

From Fig. 9, it is seen that the circumferential location of the tangential shear stress intensity coefficient approaches a limit of approximately 57° as the friction coefficient increases.

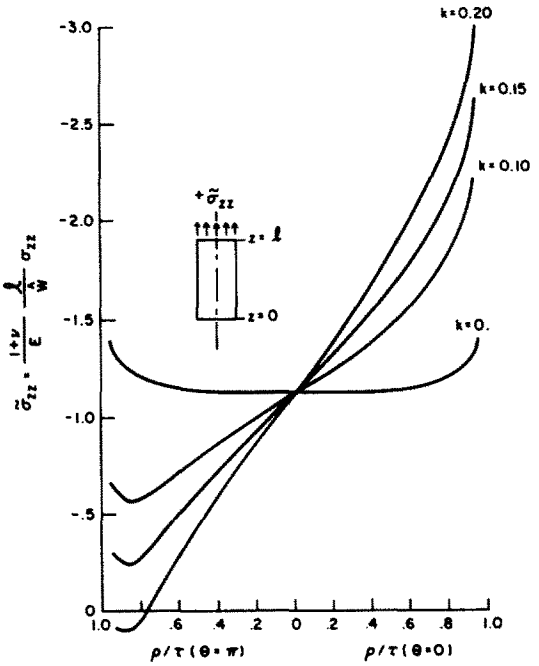

Fig. 7. Normal stress distribution at $z = l$ for various friction coefficients. $l/D = 2$, $\nu = 0.25$.

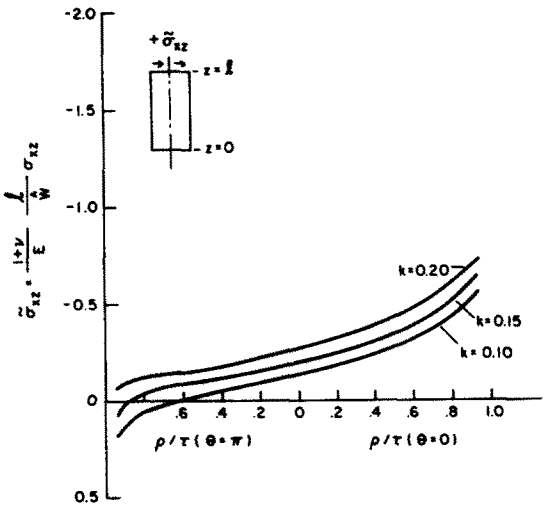

Fig. 8. Shear stress distribution at $z = l$ for various friction coefficients. $l/D = 2$, $\nu = 0.25$.

Table 1. Radial stress intensity coefficient at $\theta = 0°$, 180° for various friction coefficients. $l/D = 1$, $\nu = 0.25$

k	$K_r(0°)$	$K_r(180°)$
0.0	−0.1739	−0.1739
0.15	−0.07892	−0.2696
0.2	−0.04781	−0.3018
0.3	0.01367	−0.3665
0.5	0.1339	−0.4964
1.0	0.4335	−0.8254

Table 2. Tractions at the ends of the cylinder. $l/D = 1$, $\nu = 0.25$, $k = 0.15$

	$\theta = \pi$							$\theta = 0$						
$\rho/r =$	0.94	0.84	0.68	0.52	0.36	0.20	0.04	0.04	0.20	0.36	0.52	0.68	0.84	0.94
σ_{xz} $(z = l)$	0.2124	0.0770	−0.0150	−0.0809	−0.1348	−0.1808	−0.2215	−0.2397	−0.2742	−0.3084	−0.3453	−0.3915	−0.4633	−0.5299
σ_{zz} $(z = l)$	−0.8678	−0.7895	−0.8535	−0.9324	−1.005	−1.0602	−1.1141	−1.1402	−1.1958	−1.2614	−1.3450	−1.4675	−1.6924	−2.0466
σ_{zz} $(z = 0)$	−1.7222	−1.6853	−1.5510	−1.4565	−1.3860	−1.3298	−1.2801	−1.2553	−1.2031	−1.1429	−1.0696	−0.9761	−0.8642	−0.8520

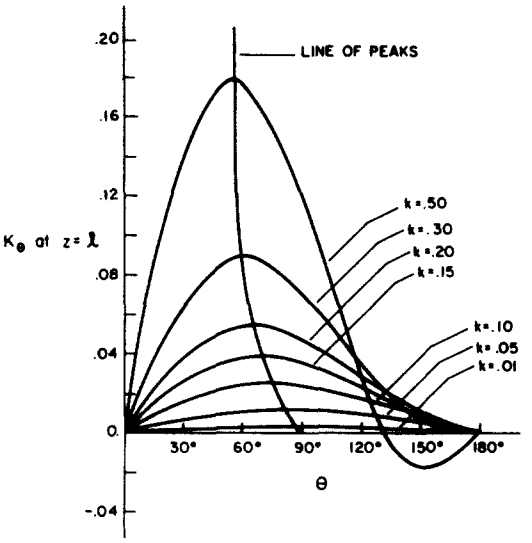

Fig. 9. Tangential stress intensity coefficient vs θ. Several friction coefficients. $l/D = 1$, $\nu = 0.25$, $z = l$.

For small values of the friction coefficient, the location of the peak approaches 90°, and the magnitude decreases to zero as the friction coefficient tends to zero.

Acknowledgements—This work was supported in part by the U.S. Air Force Office of Scientific Research under contract #F49620-79-C-0221. The project monitor was Col. Joseph D. Morgan. All numerical computations were performed using the facilities of the University of Connecticut Computer Center.

REFERENCES

1. S. L. Rice and R. Solecki, Final scientific report to United States Air Force. Air Force Office of Scientific Research. *Wear of Homogeneous and Composite Materials Under Conditions of Repeated Normal and Sliding Impact* (1977).
2. G. M. de La Penha, The end problem for a torsionless hollow circular elastic cylinder. Doctoral dissertation, University of Houston (1968).
3. J. P. Benthem and P. Minderhoud, The problem of the solid cylinder compressed between rough rigid stamps. *Int. J. Solids Structures* **8**, 1027–1042 (1972).
4. A. R. Zak, Elastic analysis of cylindrical configurations with stress singularities. *J. Appl. Mech., Trans. ASME* **39**, 501–506 (1972).
5. G. D. Gupta, The analysis of the semi-infinite cylinder problem. *Int. J. Solids Structures* **10**, 137–148 (1974).
6. J. S. Solecki and J. L. Swedlow, Elastic stress analysis of constrained cylinders by a special finite element method. *Int. J. Solids Structures* **16**, 959–968 (1980).
7. J. C. Yao, Long cylindrical tube subjected to two diametrically opposite loads. *Aero. Quart.* **20**, 365–381 (1969).
8. G. P. Steven, A non-axisymmetric cylindrical contact problem. *Int. J. Engng Sci.* **15**, 95–103 (1977).
9. F. Erdogan, G. D. Gupta and T. S. Cook, The numerical solutions of singular integral equations. *Methods of Analysis and Solutions to Crack Problems* (Edited by G. C. Sih), Noordhoof, Leyden (1972).
10. R. A. Eubanks and E. Sternberg, On the completeness of the Boussinesq–Papkovich stress functions. *J. Rat. Mech. Anal.* **5**, 735–746 (1956).
11. R. J. Conant, The effects of sliding friction on the stresses and deformations of an elastic, solid, right circular cylinder pressed against a rough rigid surface. doctoral dissertation, The University of Connecticut (1980).
12. J. D. Achenbach, *Wave Propagation in Elastic Solids*. North-Holland, Amsterdam (1975).
13. G. P. Tolstov, *Fourier Series*. Dover Publications, New York (1962).
14. R. Solecki and R. J. Conant, Stress singularities at the edge of a cylindrical slider. *J. Appl. Mech. (Brief Notes)* **49**, 224–225 (1982).